Numerical study of the effect of the type of fuel on pollutant emissions in a diesel engine

S. Kabar & M. Kadja
LEAP Laboratory, Département de Génie Mécanique,
Université Mentouri, 25000 Constantine, Algeria

Abstract

In order to minimise the planet heating observed during recent years, many studies have been undertaken on the different factors responsible for this atmospheric pollution, among which are the studies of the physical and chemical phenomena occurring in combustion. In order to diminish the polluting gases emanating from I.C. engines, the idea is to lower fuel consumption while maintaining engine performance. In this context, we numerically calculated the concentration of different polluting species (CO, CO_2, HC and NO) by using the commercial programme KIVA2 for four fuels (DF2, C_8H_{18}, C_7H_{16}, and $C_{14}H_{13}$) in a direct injection diesel engine of type CMT/FL912. The Zeldovich chemical reactions for the formation of NO, the global fuel oxidation reaction and the equilibrium reactions contributing to the formation of pollutants have been introduced. A comparison of polluting species of various fuels obtained after combustion is presented.
Keywords: KIVA2 code, diesel engine, turbulent combustion, polluting gases, fuels.

1 Introduction

During the last two decades, energy demand in the world has increased. The prices of fossil fuels have increased and the ecological repercussions due to the emissions of polluting gases CO, CO_2 and NO_X have become worrisome, particularly the rate of CO_2 in the atmosphere which is continuously increasing and which results in global heating. The shortage and the depletion of conventional energy resources are also one of the major concerns for western countries. This has incited scientists to develop alternate fuels such as bio fuels,

WIT Transactions on Engineering Sciences, Vol 59, © 2008 WIT Press
www.witpress.com, ISSN 1743-3533 (on-line)
doi:10.2495/AFM080121

LPG (liquid petroleum gas), GNV (vehicle natural gas) and finally synthesis liquid fuels.

The objective of our work is to numerically study the emissions of polluting gases CO, CO_2, HC (unburned hydrocarbons) and NO from a diesel engine. A comparison has been made between various fuels for the mass fractions of the polluting gases. The study was conducted using the code KIVA II. The latter solves simultaneously the equations governing the mechanics of fluids, the heat transfer, the mass transfer and the chemistry occurring during combustion inside an engine.

2 Mathematical formulation

The prediction of the properties of reactive flows due to the combustion of liquid fuel jets in diesel engines must take into account the liquid phase and the gaseous phase in the flow field. Several approaches have been suggested to model the discontinuity of the gas-liquid phases [1].

Among them, the statistical Eulerian-Lagrangian approach [2], which is used in the Kiva II code, and which consists of describing the field of flow of the gaseous phase in Eulerian coordinates by the averaged Navier-Stokes equations and the turbulent model equations. The liquid droplets field is described in a Lagrangian formulation, which has the advantage of being able to take into account the temperatures and the momentum of representative samples of all the different drops possessing the same characteristics (position, velocities, size, temperature, etc.) [4]; thereby avoiding the modelling of effective diffusion coefficients of mass, momentum and energy of the liquid.

The influence of the liquid phase on the gaseous phase is handled by introducing the source terms, due to the coupling of the liquid gas phases, in the balance equations of the Eulerian phase.

2.1 Chemical reactions

In the present study, four fuels have been chosen: these being $C_{14}H_{30}$ "n-tetradecane", the DF2 "diesel fuel 2" which is represented by the $C_{12}H_{26}$ "dodecane" in the chemical reaction, the C_7H_{16} "n-heptanes" and finally C_8H_{18} "iso-octane". Their global chemical reactions are:

$$\begin{aligned} 2\,C_{14}H_{30} + 43\,O_2 &\longrightarrow 28\,CO_2 + 30\,H_2O \\ 2\,C_{12}H_{26} + 37O_2 &\longrightarrow 24\,CO_2 + 26\,H_2O \\ 2\,C_8H_{18} + 25O_2 &\longrightarrow 16\,CO_2 + 18\,H_2O \\ C_7H_{16} + \quad 7O_2 &\longrightarrow \quad 7\,CO_2 + 8\,H_2O \end{aligned} \tag{1}$$

2.2 Equilibrium reactions

$K_r(T)$ is the equilibrium constant of the n°r reaction, which is assumed to depend only on the temperature:

$$K_r = \exp\left(A_r \ln T_A + \frac{B_r}{T_A} + C_r + D_r T_A + E_r T_A^2 \right) \quad (2)$$

where A_r, B_r, C_r and D_r are constants, and $T_A=T/1000$.

We have considered the seven following reactions:

Table 1: Value of A_r, B_r, C_r and D_r.

Reaction n° r	A_r	B_r	C_r	D_r	E_r
$H_2 \leftrightarrow 2H^\circ$	0.990207	-51.7916	0.993074	-0.343428	0.0111668
$O_2 \leftrightarrow 2O^\circ$	0.431310	-59.6554	3.503350	-0.340016	0.0158715
$N_2 \leftrightarrow 2N^\circ$	0.7947009	-113.2080	3.168370	-0.443814	0.0269699
$O_2 + H_2 \leftrightarrow 2OH^\circ$	-0.652939	-9.8232	3.930330	0.163490	-0.0142865
$O_2 + 2H_2O \leftrightarrow 4OH^\circ$	1.158882	-76.8472	8.532155	-0.868320	0.0463471
$O_2 + 2CO \leftrightarrow 2CO_2$	0.980875	68.4453	-10.5938	0.574260	-0.0414570
$O_2 + N_2 \leftrightarrow 2NO$	0.000000	-10802	0.14	$7.2\ 10^{-5}$	0.0000000

2.3 Kinetic reactions

We take into account the kinetics of the reaction towards the equilibrium by a reaction rate given by the Arrhenius' law:

$$\dot{\omega}_r = k_{fr} \prod_{m=1}^{nsp} \left(\frac{\rho_m}{W_m} \right)^{a'_{mr}} - k_{br} \prod_{m=1}^{nsp} \left(\frac{\rho_m}{W_m} \right)^{b'_{mr}} \quad (3)$$

k_{fr} and k_{br} are the reaction rate constants respectively for both directions of reaction n°r.

Zeldovich's chemical mechanism for the formation of NO is taken into account by introducing the coefficients and the equilibrium constants of the following chemical reactions into the KIVA II code:

$O_2 + 2N_2 \rightleftharpoons NO + 2N$

$k_{fr} = 1.558.10^{14} \exp(6.76.10^4/T)$

$k_{br} = 7.500.10^{12}$

$N_2 + 2OH \rightleftharpoons 2NO + 2H$

$k_{fr} = 2.648.10^{10} \exp(5.94.10^4/T)$

$k_{br} = 1.600.10^{9} \exp(1.96.10^4/T)$

$N_2 + 2O_2 \rightleftharpoons 2NO + 2O$

$k_{fr} = 2.132.10^{14} \exp(5.70.10^4/T)$

$k_{br} = 0.0$

3 Numerical methods

The temporal discretisation is a discrete sequence of times t^n ($n=0,1,2....$). The interval of time $\Delta t^n = t^{n+1} - t^n$ is the step of time and n is the number of cycles. In the KIVA II code, the cycle takes place in three stages or phases. Phase A and Phase B constitute the Lagrangian calculation where the grid nodes

move at the same speed as the fluid. There is thus no convection through the sides of the grid cells. So, during this first phase none of the convective terms of the aerodynamics equations are taken into account. In phase C, the field of flow is frozen and the grid nodes are returned to the new positions prescribed by the user with the aim of calculating the compression and the expansion. This remeshing is realized by transporting by convection the various quantities through the boundaries of the control volumes when these are moved to their new positions.

4 Results and discussion

The simulation has been applied to the combustion chamber of the diesel engine CMT FL912 that is mounted on the tractor CIRTA C6807 manufactured in Constantine, Algeria by the national company SONACOM. Its 68 KW power is reached through a rotation speed of 2300rpm. For the current work, we have used the engine regime which is 1600rpm rotation speed corresponding to the maximum couple. The walls are maintained at constant temperatures, the initial time step is dti = 10^{-7}s, the tolerances for the convergence of the method of conjugated residues for the implicit terms diffusion of pressure gradient epsp = 10^{-4}, chemical species epsy, momentum epsv, heat epst and kinetic energy epsk are all equal to 10^{-3}.

Table 2: Characteristics of the engine.

Cylinder diameter	100 mm
Piston course	120 mm
Distance between cylinder head and piston surface at TDC (squich)	1.8 mm
Length of the connecting rod	216 mm
Injector diameter	0.285 mm
Engine speed	1600 tr/min
Injection period	12°
Injection Mode	Injection according to a half sinusoid
Rate of injection	50 cm^3/s
Injection pressure	400 bars
Injection temperature	313°K (40°C)
Air temperature	400 K
Total number of injected particles	2000
Inclination angle of injector orifice	60°
Thickening angle of fuel jet	10°
Cylinder wall temperature	400K
Piston wall temperature	400K
Temperature of cylinder head	400K
Initial density of oxygen	2.4257×10^{-4} g/cm^3
Initial density of nitrogen	7.9851×10^{-4} g/cm^3

The numerical grid used in this study contains 25 cells in radial direction (NX=25), 1 cell in the azimuthal direction (NY=1) and 40 cells in the axial direction (NZ=40). At the beginning of the calculation (at -90°), the grid starts with 40 cells in the axial direction (NZ=40). During the compression phase, cells are compressed as the piston approaches the top of cylinder (top dead center TDC), until a minimal number of cells (which is two) between the cylinder head and the top surface of the piston is reached.

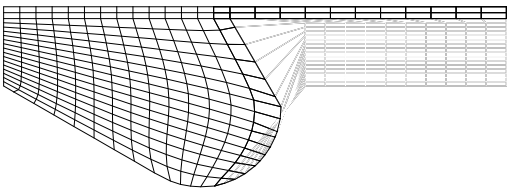

Figure 1: The grid mesh at 0.0068 degrees before the top of the cylinder.

4.1 Formation of pollutants

4.1.1 Unburned hydrocarbons

The curve of fuel consumption (Fig. 2) by the oxygen is the same for the various fuels. The fuel begins to evaporate as soon as the first injected drops in the combustion chamber from the advanced angle of injection until the evaporation of part of the fluid that corresponds to the maximum of the curve. From this point onwards the first free radicals start to form to provoke the immediate explosion of the fuel at around the top of the cylinder (TDC). At that moment, the curve decreases then becomes asymptotic to a value which corresponds to unburned hydrocarbons which are due to the short duration of the combustion at

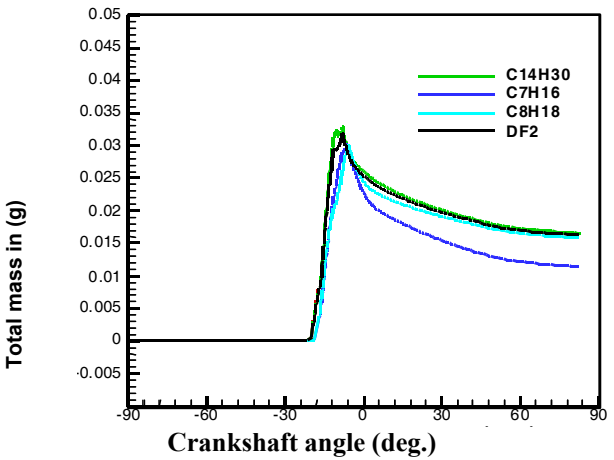

Figure 2: Evolution of total fuel mass as a function of Crankshaft angle for various fuels.

about 12° (Fig. 2), and which is shorter than the period of self-ignition necessary for the fuel to completely oxidize, and by the adhesion of droplets to the walls of the combustion chamber to evaporate which are at a lower temperature (Fig. 3). The unburned hydrocarbons are then chased away by exhaust gases.

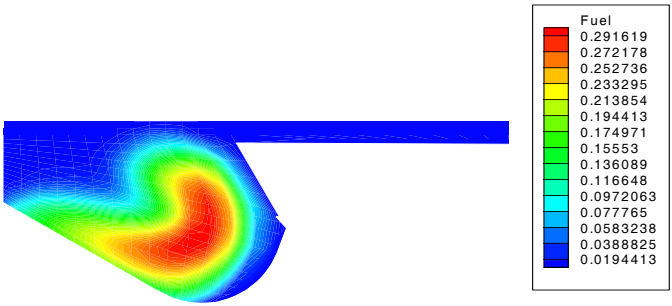

Figure 3: Contours of the mass fractions of the consumption of the fuel at the position (–5°) before the TDC for DF2.

4.1.2 Carbon dioxide

The carbon dioxide begins to form as soon as fuel ignition (Fig. 4) in the flame zone by the chemical kinetic mechanism of hydrocarbon oxidation at 12° before TDC (Fig. 5). The total mass of CO_2 increases quickly till the end of the ignition then continues to form in a slower way by the chemical mechanism of equilibrium of CO oxidation and of CO_2 dissociation into CO during the expansion phase up to a maximal value (Fig. 4).

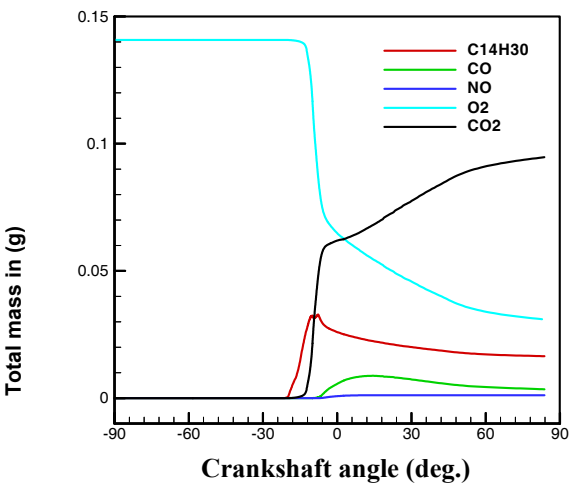

Figure 4: Evolution of total masses of polluting gases as a function of the crankshaft angle for the fuel $C_{14}H_{30}$.

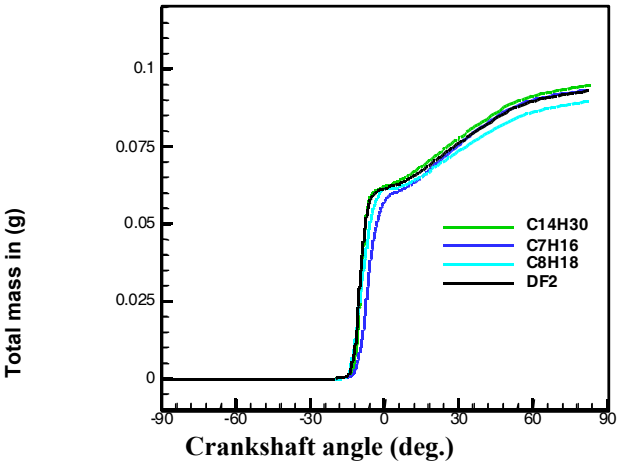

Figure 5: Evolution of CO_2 mass as a function of the crankshaft angle for various fuels.

4.1.3 Carbon monoxide

The carbon monoxide forms well far from the flame front (Fig. 4), by the fact of the lack of oxygen. The thermodynamic equilibrium of CO_2 dissociation and the reaction of CO_2 and H_2 will result in a mass that represents 20% of the mass of fuel at the maximum point at 15 ° after TDC (Fig. 6). This quantity will decrease during the expansion phase because of its transformation to CO_2 until a negligible value is reached (Fig. 4).

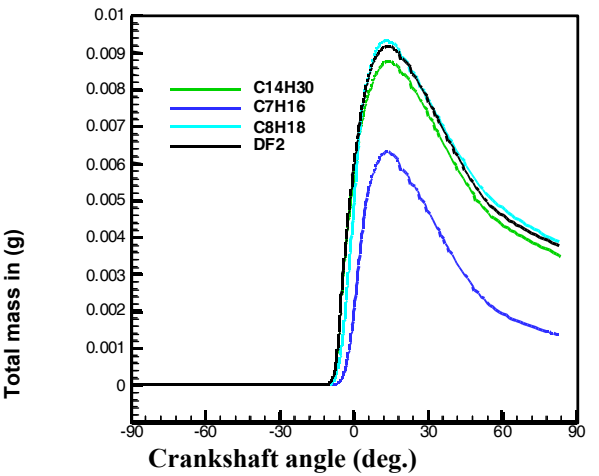

Figure 6: Evolution of the total masses of carbon monoxide according to the swing angle for the various fuels.

4.1.4 Nitrogen oxide

The formation of NO begins at 5 ° before TDC far from the flame front because of the lack of oxygen (Fig. 7). The curve undergoes an exponential jump, which confirms that the formation of NO essentially results from the chemical kinetics. NO then reaches a maximal value at the end of combustion, which will remain constant until the end of the expansion. We can deduce that the formation of NO takes place at high temperatures (fig. 7).

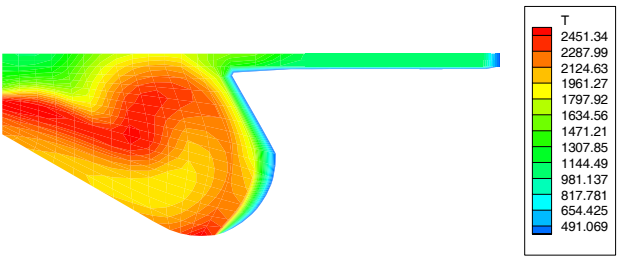

Figure 7: Isotherms at the position (–5°) before the TDC for C7H16.

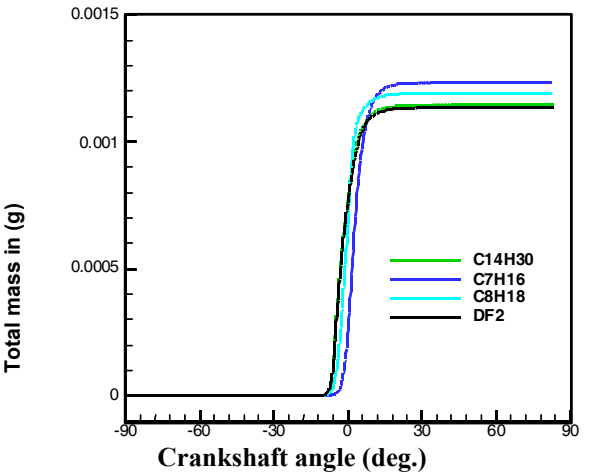

Figure 8: Evolution of nitrogen oxide mass as a function of the crankshaft angle for various fuels.

4.2 Comparison of the results for the various fuels

4.2.1 Unburned hydrocarbons

The C_7H_{16} (n-heptane) has the least unburned evaporated mass which is 0.011g, and which represents 36% of the evaporated mass, whereas $C_{14}H_{30}$ (n-tetradecane), DF2 and C_8H_{18} (isooctane) have almost the same unburned

hydrocarbons evaporated mass of 0.015g. Consequently C_7H_{16} (n-heptane) emits the least unburned hydrocarbons.

4.2.2 Carbon dioxide

The curve of CO_2 formation (Fig. 4) is the same for the four fuels. The mass of the carbon dioxide, CO_2 (Fig. 5) emitted by various fuels, is practically the same. The total mass of CO_2 is between 0.08g and 0.09g.

4.2.3 Carbon monoxide

The curve of CO (Fig. 6) is similar for the four fuels. The mass of the carbon monoxide CO emitted at the end of combustion by C7H16 (n-heptane) (Fig. 2) is 0.0013g and is sharply lower than those of the other fuels. We notice that the curves of CO for C14H30, Df2 and the C8H18 (isooctane) are identical. The mass emitted is 0.003g.

4.2.4 Nitrogen oxide

The curve of formation of NO is similar for the four fuels (Fig. 8). We notice in Fig. 5 that the combustion of $C_{14}H_{30}$ (n-tetradecane) and DF2 emits less nitrogen oxide NO gases, they have each a mass of 0.0114g at the end of the cycle whereas the combustion of the C_7H_{16} (n-heptane) produces more NO; its mass is 0.00122g.

5 Conclusion

The numerical bi-dimensional study of the type of fuel on the polluting emissions emanating from a diesel engine has been achieved by using the KIVA II code. The kinetic chemical mechanisms and the balance of the formation of various pollutants have been implemented in the code.

The results obtained for the four fuels give us the following comparative analysis:

- The four fuels produce at the end of the combustion the same density of carbon dioxide.
- The C_7H_{16} (n-heptane) emits less unburned hydrocarbons because of the weak number of the carbon atoms. The energy of atoms connection is less important than the other fuels.
- In spite of the lower number of carbon atoms, the emissions of C_8H_{18} (isooctane) polluting gases is the same as for the emissions of the DF2 and the $C_{14}H_{30}$ (n-tetradecane).
- The emissions of carbon dioxide for the four fuels are very close because of the temperature at the end of combustion, which is identical for all.
- The emissions of carbon monoxide are less important for C_7H_{16} (n-heptane) because the CO_2 residential time is shorter than the other fuels (ignition delay shorter).
- The emissions of nitrogen oxide are less important for $C_{14}H_{30}$ (n-tetradecane) and the DF2.

References

[1] R. Borghi et M. Champion, Modélisation et théorie des flammes: EDITION TECHNIP, Paris, 2000
[2] T. J. Chung, Computational fluid dynamics, Cambridge University Press, 2002
[3] Roland Borghi, Michel Destriau et Gérard De Soete, La combustion et les flammes: EDITION TECHNIP, Paris, 1995.
[4] A. A. Amsden, P. J. ÕRourke, T. D. Butler, KIVA-II: A Computer Program for Chemically. Reactive Flows with Sprays: LA-11560-MSUC-96, Los Almos, May 1989